Mesoporous Materials

DOI: 10.1002/anie.201002104

Chitin–Silica Nanocomposites by Self-Assembly**

Bruno Alonso and Emmanuel Belamie**

Self-assembly of chemical entities is at the basis of many biological processes and increasingly in materials syntheses.[1–4] Self-assembled surfactants[5] and block copolymers[6] are widely and successfully used to prepare ordered hybrid and mesoporous materials with outstanding properties.[3,7–9] A strong interest also rises for energy-saving chemical processes and reactants from renewable resources.[10,11] Self-assembled biomacromolecules and other biological objects have been used previously as liquid-crystal templates for the formation of mesoporous silica.[12–14] Herein we present a novel and versatile colloid-based approach for the large-scale synthesis of a new family of hybrid bioorganic–inorganic nanocomposites with an unprecedented control in texture and morphology. This approach combines the self-assembly properties of polysaccharide chitin nanorods,[15] with the flexibility of sol–gel processes involving siloxane oligomers.[16,17] The resulting optical and mechanical properties of the chitin–silica nanocomposites can be tuned by varying the chitin volume fraction ϕ_{CHI}. Nanorod alignment inside these materials was achieved under moderate magnetic fields (9 T), generating highly oriented textures and providing an alternative method to that developed for surfactant-templated materials.[18] Furthermore, sol–gel chemistry is amenable to a variety of processing techniques such as spray-drying, which allowed us to prepare micrometer-size chitin–silica particles with variable porosity in the calcined replicas.

Our approach consists in the formation and processing of a stable suspension containing two colloids, α-chitin nanorods and siloxane precursors, both in a dispersed state. This is a challenging issue owing to differences in stability and reactivity of the colloids. Chitin nanorods purified from shrimp shells ($L = 260 \pm 80$ nm, $D = 23 \pm 3$ nm)[15] are bundles of monocrystals ($D = 3.2 \pm 0.6$ nm) with amino groups at their surface (Figure 1 a). They are stably dispersed in water by electrostatic repulsions in slightly acidic conditions.[15] The simple addition of silica precursors would lead to uncontrolled chitin/silica precipitation owing to electrostatic interactions and/or rapid siloxane condensation. To avoid this, we prepared mixed alcoholic suspensions of the chitin nanorods with siloxane oligomers through repeated solvent exchange cycles. The siloxane oligomers were formed by controlled acid-catalyzed hydrolysis with a hydrodynamic diameter of about 4 nm and a degree of siloxane condensation c of 0.75 (Figure 1 a). The resulting clear to translucent suspensions (depending on chitin concentration) are stable over a long period of time (several months).

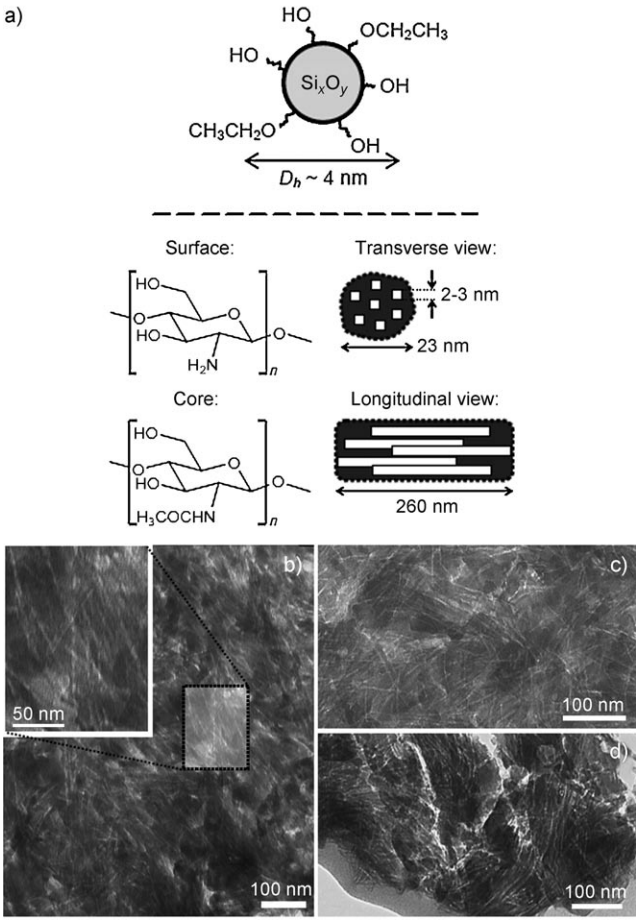

Figure 1. a) Representation of the siloxane oligomers (upper panel), and of the chitin nanorods (core: poly[β-(1→4)-2-acetamido-2-deoxy-D-glucopyranose]) as bundles of monocrystals with amino groups at their surface (lower panel). The colloid sizes were estimated by DLS and TEM. b–d) TEM analysis: b) bulk nanocomposite ($\phi_{CHI} = 0.28$); spray-dried microparticles ($\phi_{CHI} = 0.28$) before (c) and after (d) calcination (porous replicas).

Upon evaporation, the colloidal suspension shows a marked increase in viscosity and turbidity, which is accompanied by a gradual rise in optical birefringence. In a standard procedure, the resulting pasty mixture was cast and further dried overnight (348 K), yielding hard bulk materials with condensation degrees c in the expected range of 0.8–0.9.[19] Preliminary compression tests show that the elastic mechan-

[*] Dr. B. Alonso, Dr. E. Belamie
Institut Charles Gerhardt de Montpellier ICGM
UMR 5253 CNRS-ENSCM-UM2-UM1
8 rue de l'Ecole Normale, 34296 Montpellier cedex 5 (France)
Fax: (+33) 4-6716-3470
E-mail: bruno.alonso@enscm.fr
emmanuel.belamie@enscm.fr

[**] T. Cacciaguerra (TEM/SEM imaging), Dr. F. Di Renzo (N_2 sorption analyses), and Dr. L. Vachoud (compression–strain experiments) are acknowledged for their help.

Supporting information for this article is available on the WWW under http://dx.doi.org/10.1002/anie.201002104.

ical properties could be enhanced upon addition of chitin in an intermediate range of ϕ_{CHI} around 0.3 (see the Supporting Information). Beyond, the pelleted materials have increasing plasticity. This evolution of the mechanical properties with ϕ_{CHI} is consistent with changes in the extent of the chitin monocrystal coating by siloxane oligomers as discussed below. In the bulk, the polycrystalline chitin nanorods are preserved and well-dispersed in the final siloxane network (Figure 1). The presence of chitin nanorods inside the nanocomposites was confirmed by ^{13}C and ^{15}N solid-state NMR, FTIR spectroscopy, X-ray diffraction, and TEM (representative micrographs shown in Figure 1 b–d; for more details, see the Supporting Information). These samples exhibit optical birefringence related to local ordering of the chitin nanorods, but within small independent domains (ca. 100 μm). By keeping the samples under a magnetic field **B** throughout solvent evaporation and across the sol-gel transition, the resulting materials showed homogenous long-range (several centimeter) alignment of the chitin nanorods perpendicular to **B**. This preferred orientation, which is most likely related to cooperative effects previously observed with chitin nanorods in aqueous dispersions,[15] is preserved after calcination (Figure 2).

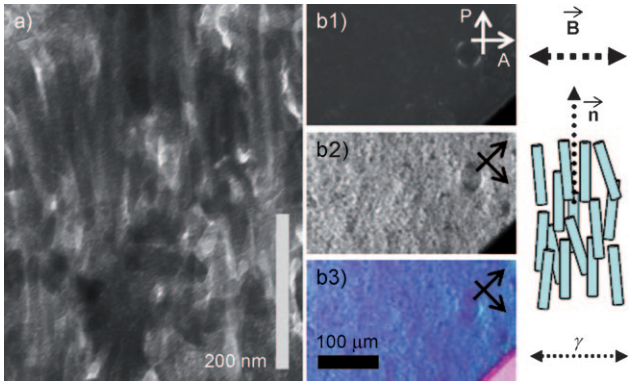

Figure 2. Magnetic field alignment: a) TEM micrograph of a mesoporous sample with aligned pores (initial $\phi_{CHI} = 0.28$). b) Series of representative polarized-light micrographs of the same sample as (a) for different orientations with respect to the directions of both the magnetic field **B** and the polarizers (crossed arrows: P = polarizer, A = analyzer). The strong homogenous birefringence of the uniaxially oriented sample is revealed by a fourfold increase in light intensity after a 45° rotation (b1 → b2). b3) Blue color obtained after introducing a first-order λ retardation plate (**γ** = slow axis direction), indicating that the structure is aligned along **n** perpendicular to the magnetic field direction **B**.

Spray-dried chitin–silica particles and their related calcined porous replicas have an overall spheroid shape (Figure 3) and mean diameters in the 2.2–2.5 μm range (see the Supporting Information). Increasing ϕ_{CHI} resulted in a visible roughening of the particle surface, with elongated rods separated by voids (10–100 nm) visible at high ϕ_{CHI} (Figures 3 and 4). The rods have dimensions ($D = 26 \pm 6$ nm, $L = 240 \pm 45$ nm) very close to those of the extracted chitin nanorods. This result suggests that the latter are coated by siloxane

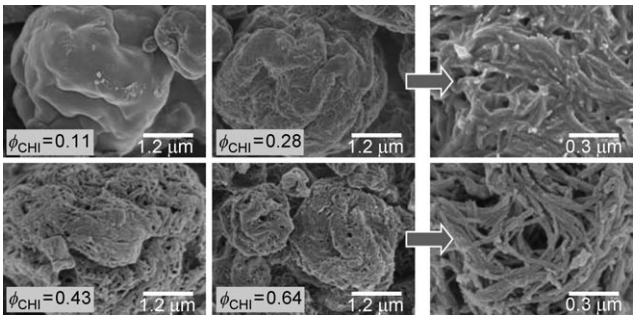

Figure 3. SEM analysis of spray-dried microparticles, showing variations in morphology and surface roughness as a function of the initial chitin volume fraction ϕ_{CHI} (here porous replicas). The two micrographs on the right correspond to $\phi_{CHI} = 0.28$ and 0.64, and show the variations in surface at a higher magnification. For additional data, see the Supporting Information.

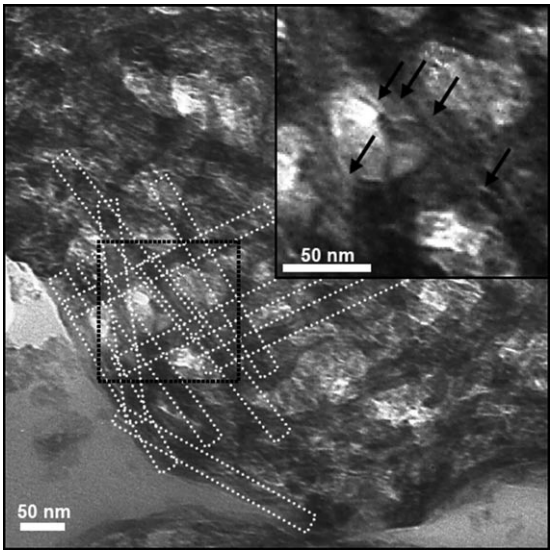

Figure 4. TEM analysis of spray-dried microparticles obtained with high initial chitin volume fractions (here $\phi_{CHI} = 0.64$, porous replica). The sample is formed by entangled rods of silica (white dashed rectangles) separated by voids (10–100 nm). These rods come from the initial chitin nanorods represented by the rectangles (23×260 nm^2). Inside the silica rods, the imprint of the chitin monocrystals (2–3 nm wide) can be distinguished (black arrows in the zoomed area).

oligomers to form hybrid rods, which are transformed into porous silica structures in the calcined samples (Figures 1 c,d and 4).

Calcination reinforces the siloxane network ($c > 0.9$) and generates porosity. The porous volume fraction ϕ_{POR} is essentially proportional to ϕ_{CHI} (Figure 5 a), whilst the specific surface area S_{BET} shows a gradual increase in the 0–450 m^2 g^{-1} range (Figure 5 b). The higher porosity of the spray-dried microparticles compared to the bulk materials probably comes from the formation of voids as mentioned above. All N_2 sorption isotherms are characteristic of mesoporous samples (IUPAC Type IV), but changes in the shape of the hysteresis loop reveal a shift from moderately connected

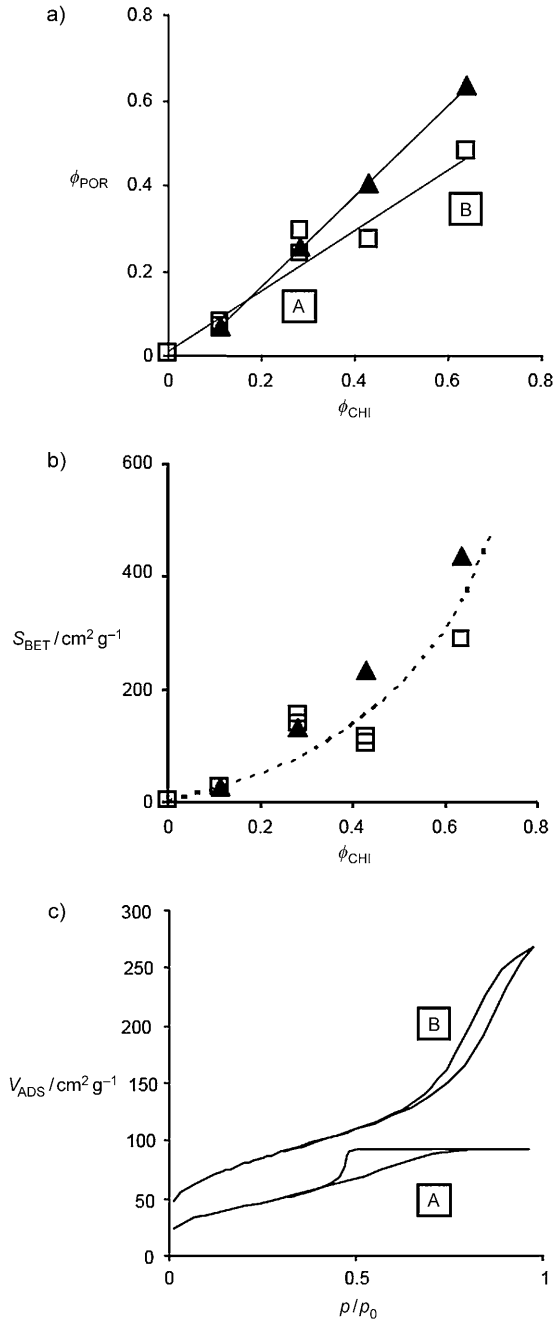

Figure 5. N_2 porosimetry: a) Pore volume fraction ϕ_{POR} as a function of chitin volume fraction ϕ_{CHI} for calcined samples: bulk materials (□) and spray-dried microparticles (▲). b) Specific surface area S_{BET} as a function of ϕ_{CHI} for calcined samples: bulk materials (□) and spray-dried microparticles (▲). The broken line indicates and corresponds to modeled S_{BET} values obtained using variable ϕ_{CHI}, a density of silica of 2, and dispersed parallelepiped pores of dimensions $10\times10\times260$ nm^3. c) Typical isotherms (adsorbed volume V_{ADS} versus relative pressure p/p_0) obtained for calcined gels, showing a transition from IUPAC type H2 ($\phi_{CHI}<0.3$) to H3 hysteresis loop ($\phi_{CHI}>0.4$). No microporosity is found for any isotherms using the *t*-plot transformation.

mesopores at $\phi_{CHI}<0.3$ to a more complex and opened porosity at $\phi_{CHI}>0.4$ (Figure 5c). At $\phi_{CHI}<0.3$, the estimated pore diameters (3–5 nm) are very close to the lateral dimensions (2–3 nm) of the straight elongated structures observed by TEM (Figure 1d and 4). This strongly suggests that siloxane oligomers not only cover the external surface of the nanorods, but actually coat each individual chitin monocrystal. Beyond a critical ϕ_{CHI}* value, which is tentatively estimated to be 0.2–0.4, the incomplete coating of chitin monocrystals would lead to interconnections between pores, resulting in higher pore diameters as observed for $\phi_{CHI}>0.4$ (4–13 nm). To some extent, this may also account for increased plasticity of the nanocomposites beyond an optimal chitin volume fraction at around 0.3.

The observed textures and the related properties indicate a high dispersion level of the chitin nanorods in the initial alcoholic suspension, which was preserved throughout the processing steps. ^{1}H spin diffusion studies ($\phi_{CHI}=0.64$) confirm the absence of a phase separation above the 100 nm scale, and the presence of a chitin–siloxane interface defined at the nanometer scale (see the Supporting Information). Furthermore, even after spray-drying, in which fast solvent evaporation quenches the system out of equilibrium, chitin nanorods are not aggregated. Converging elements therefore suggest the existence of a soft attractive interaction between the siloxane oligomers and the chitin surface, which might result in the formation of chitin–siloxane particles during the early stages of the synthesis. This hypothesis is supported by the presence at chitin surfaces of a high density of amino groups known to interact with siloxane species and to favor their condensation,[20,21] and by the possible implication of chitin in biosilification.[22] Although the rise in birefringence during evaporation showed no discernable threshold that is indicative of a first-order transition, the chitin–siloxane suspensions clearly behave as a mesophase, with liquid-like local order comparable to a nematic phase.

In summary, our novel approach takes advantage of the properties of elongated chitin nanorods in suspension and of the versatility of sol–gel processes to design chitin–silica nanocomposites and mesoporous materials. The formation mechanism is governed by chitin self-assembly coupled with chitin–siloxane soft attractive interactions, which bears similarities with cooperative and dynamical template mechanisms proposed earlier.[23,24] The stability of the alcoholic mixed suspensions gives remarkable opportunities to prepare materials with adjustable volume fractions, spatial ordering, and morphologies. Further work is in progress, notably to better describe the structure–texture relationships, and to fully explore the opportunities in materials processing (membranes, spheres, fibers).

Experimental Section

Aqueous suspensions of chitin nanorods in 10^{-4} M HCl were prepared following a procedure described elsewhere,[15] based on the hydrolysis of chitin in 4 M HCl, followed by the purification of the nanorods. In parallel, an alcoholic solution containing siloxane oligomers was obtained by mixing and refluxing tetraethyl orthosilicate (TEOS; 0.1 mol), an acidic aqueous solution (0.1 M HCl), and ethanol with molar proportions TEOS/H_2O/EtOH 1:2:2 for 4 hours. The chitin suspension and siloxane solution were then mixed in absolute ethanol. The reactant proportions were chosen to reach the water–ethanol azeotrope composition and a given chitin volume fraction ϕ_{CHI} in the final nanocomposites. After vigorous stirring, a homoge-

neous solution was obtained. The mixture was evaporated until a paste is obtained, and the same initial amount of ethanol was added. This solvent-exchange cycle was repeated three times for water removal.

Processing: In a standard procedure, ethanol was further evaporated and the final paste dried in an oven for about 15 hours (348 K). For magnetic field alignment, evaporation proceeded slowly (about 1 month) in vertical tubes placed in a NMR magnet ($B =$ 9.4 T). The microparticles were obtained by spray-drying the suspensions under dry nitrogen in a Büchi 290 mini-spray dryer. The chitin content estimated from elemental analyses and expressed as ϕ_{CHI} lies within 10 % of the target value. Mesoporous samples were obtained by calcination (8 hours, 823 K). Siloxane condensation degrees c were calculated from ^{29}Si solution- and solid-state NMR spectra.

Received: April 9, 2010
Revised: June 16, 2010
Published online: September 23, 2010

Keywords: chitin · hybrid materials · mesoporous materials · nanoparticles · sol–gel processes

[1] G. M. Whitesides, B. Grzybowski, *Science* **2002**, *295*, 2418.
[2] I. W. Hamley, *Angew. Chem.* **2003**, *115*, 1730; *Angew. Chem. Int. Ed.* **2003**, *42*, 1692.
[3] G. A. Ozin, K. Hou, B. V. Lotsch, L. Cademartiri, D. P. Puzzo, F. Scotognella, A. Ghadimi, J. Thomson, *Mater. Today* **2009**, *12*, 12.
[4] S. Mann, *Nat. Mater.* **2009**, *8*, 781.
[5] C. T. Kresge, M. E. Leonowicz, W. J. Roth, J. C. Vartuli, J. S. Beck, *Nature* **1992**, *359*, 710.
[6] D. Y. Zhao, J. L. Feng, Q. S. Huo, N. Melosh, G. H. Fredrickson, B. F. Chmelka, G. D. Stucky, *Science* **1998**, *279*, 548.
[7] A. Corma, *Chem. Rev.* **1997**, *97*, 2373.
[8] M. E. Davis, *Nature* **2002**, *417*, 813.
[9] Y. Wan, D. Zhao, *Chem. Rev.* **2007**, *107*, 2821.
[10] M. Eissen, J. O. Mertzger, E. Schmidt, U. Schneidewind, *Angew. Chem.* **2002**, *114*, 402; *Angew. Chem. Int. Ed.* **2002**, *41*, 414.
[11] N. Baccile, F. babonneau, B. Thomas, T. Coradin, *J. Mater. Chem.* **2009**, *19*, 8537.
[12] C. E. Fowler, W. Shenton, G. Stubbs, S. Mann, *Adv. Mater.* **2001**, *13*, 1266.
[13] E. Dujardin, M. Blaseby, S. Mann, *J. Mater. Chem.* **2003**, *13*, 696.
[14] D. Eglin, G. Moser, M. M. Giraud-Guille, J. Livage, T. Coradin, *Soft Matter* **2005**, *1*, 129.
[15] E. Belamie, P. Davidson, M. M. Giraud-Guille, *J. Phys. Chem. B* **2004**, *108*, 14991.
[16] C. J. Brinker, G. W. Scherer, Sol-Gel Science: The Physics and Chemistry of Sol-Gel Processing, Academic Press, San Diego, **1990**.
[17] L. L. Hench, J. K. West, *Chem. Rev.* **1990**, *90*, 33.
[18] S. H. Tolbert, A. Firouzi, G. D. Stucky, B. F. Chmelka, *Science* **1997**, *278*, 264.
[19] F. Devreux, J. P. Boilot, F. Chaput, A. Lecomte, *Phys. Rev. A* **1990**, *41*, 6901.
[20] N. Kröger, R. Deutzmann, C. Bergsdorf, M. Sumper, *Proc. Natl. Acad. Sci. USA* **2000**, *97*, 14133.
[21] T. Coradin, J. Livage, *Colloids Surf. B* **2001**, *21*, 329.
[22] E. Brunner, P. Richthammer, H. Ehrlich, S. Paasch, P. Simon, S. Ueberlein, K. H. van Pée, *Angew. Chem.* **2009**, *121*, 9904; *Angew. Chem. Int. Ed.* **2009**, *48*, 9724.
[23] A. Monnier, F. Schuth, Q. Huo, D. Kumar, D. Margolese, R. S. Maxwell, G. D. Stucky, M. Krishnamurty, P. Petroff, A. Firouzi, M. Janicke, B. F. Chmelka, *Science* **1993**, *261*, 1299.
[24] E. Pouget, E. Dujardin, A. Cavalier, A. Moreac, C. Valéry, V. Marchi-Artzner, T. Weiss, A. Renault, M. Paternostre, F. Artzner, *Nat. Mater.* **2007**, *6*, 434.

